ESC European Society of Cardiology

European Heart Journal - Imaging Methods and Practice (2024) **2**, 1–10
https://doi.org/10.1093/ehjimp/qyae006

ORIGINAL ARTICLE

Post-cardiac arrest temporal evolution of left ventricular function in a rat model: speckle-tracking echocardiography and cardiac circulating biomarkers

Daria De Giorgio [1], Davide Olivari [1], Francesca Fumagalli [1], Deborah Novelli [1], Marianna Cerrato [1], Francesca Motta [1], Giuseppe Ristagno [2,3], Roberto Latini [1], and Lidia Staszewsky [1,*]

[1]Department of Cardiovascular Medicine, Istituto di Ricerche Farmacologiche Mario Negri IRCCS, Via Mario Negri 2, 20156 Milan, Italy
[2]Department of Anesthesiology, Intensive Care and Emergency, Fondazione IRCCS Ca' Granda Ospedale Maggiore Policlinico, 20122 Milan, Italy
[3]Department of Pathophysiology and Transplantation, University of Milan, 20122 Milan, Italy

Received 17 October 2023; accepted after revision 30 January 2024; online publish-ahead-of-print 1 February 2024

Abstract

Aims

There is little information from experimental studies regarding the evolution of post-resuscitation cardiac arrest [post-return of spontaneous circulation (post-ROSC)] myocardial dysfunction during mid-term follow-up. For this purpose, we assessed left ventricular (LV) function and circulating cardiac biomarkers at different time points in a rat model of cardiac arrest (CA).

Methods and results

Rats were divided into two groups: control and post-ROSC rats. Eight minutes of untreated ventricular fibrillation were followed by 8 min of cardiopulmonary resuscitation. Conventional and speckle-tracking echocardiographic (STE) parameters and cardiac circulating biomarkers concentrations were assessed, at 3, 4, 72, and 96 h post-ROSC. At 3 and 4 h post-ROSC, LV systolic function was severely impaired, and high-sensitivity cardiac troponin T and N-terminal pro-atrial natriuretic peptide (NT-proANP) plasma concentrations were significantly increased, compared with control rats ($P < 0.0001$ for all). At 72 and 96 h post-ROSC, LV ejection fraction (LVEF) normalized. At 96 h, the following variables were significantly different from control rats: early trans-mitral peak velocity, 56.8 ± 3.1 vs. 87.8 ± 3.8 cm/s, $P < 0.0001$; late trans-mitral peak velocity, 50.6 ± 4.7 vs. 73.7 ± 4.2 cm/s, $P < 0.0001$; mean s′ wave velocity, 4.6 ± 0.3 vs. 5.9 ± 0.3 cm/s, $P < 0.0001$, global longitudinal strain (GLS) -7.5 ± 0.5 and vs. $-11 \pm 1.2\%$, $P < 0.01$; GLS rate (GLSR) -0.9 ± 0.4 and -2.3 ± 0.2 1/s, $P < 0.01$; and NT-proANP concentration, 2.5 (0.2; 6.0) vs. 0.4 (0.01; 1.0) nmol/L, $P < 0.01$.

Conclusion

s′ velocity, GLS, and GLSR indicated that LV systolic function was still impaired 96 h post-ROSC. These findings agree with NT-proANP concentrations, which continue to be high. Normalization of LVEF supports the use of STE for its greater sensitivity for monitoring post-CA cardiac function. Further investigations are needed to provide evidence of the post-ROSC LV diastolic function pattern.

* Corresponding author. E-mail: lidia.staszewsky@marionegri.it

Graphical Abstract

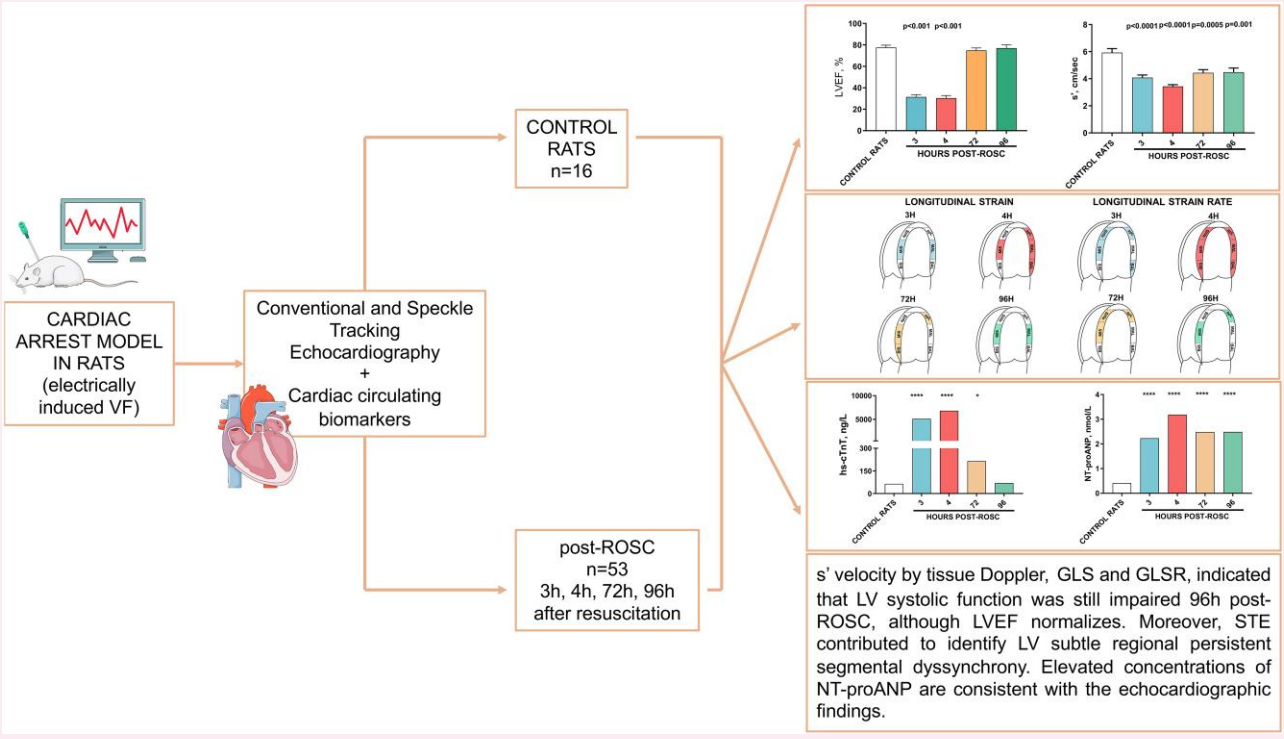

Keywords cardiac arrest • post-resuscitation • rats • left ventricular function • speckle-tracking echocardiography • conventional echocardiography • circulating cardiac biomarkers

Introduction

Cardiac arrest (CA) is a dramatic event that accounts for millions of deaths worldwide every year.[1] Even after successful cardiopulmonary resuscitation (CPR), ~60–70% of patients still die before hospital discharge mainly because of post-CA syndrome. This clinical condition is characterized principally by left ventricular (LV) and cerebral dysfunction as a consequence of a complex pathophysiological process following whole-body ischaemia during CA and the subsequent reperfusion injury post-CPR.[2]

There are different determinants to assess the severity and course of LV dysfunction, for instance, (i) pre-CA ventricular function for evaluating global ischaemia; (ii) resuscitation factors for indicating ischemia/reperfusion (I/R) injury, and also (iii) post-CA treatments.[2] Although LV dysfunction after CA has been described as mainly reversible, there is little information available on its grade of severity and evolution.[3,4] Transthoracic echocardiography is one of the most common non-invasive diagnostic tools to assess cardiac function and myocardial injury in post-CA syndrome in humans.[2] Accordingly, longitudinal experimental studies in animals using echocardiography to assess LV post-return of spontaneous circulation (post-ROSC) recovery may provide useful information to be translated into clinical practice. Previous work reported that in a rat model of ventricular fibrillation (VF) and CPR, LV ejection fraction (LVEF) and cardiac output (CO) were significantly reduced shortly after ROSC, but only one group of researchers described LV recovery after more than 4 h post-ROSC in rats.[5–8]

The purposes of this study were to characterize the post-CA LV function by conventional transthoracic echocardiography and by a more advanced echocardiographic technique, STE, together with cardiac circulating biomarkers concentrations at short-term and mid-term time points after CPR, in an experimental rat model.

Methods

Procedures involving animals were conducted at the Istituto di Ricerche Farmacologiche Mario Negri IRCCS, which adheres to the principles set out in the following laws, regulations, and policies governing the care and use of laboratory animals: Italian Governing Law (D.lgs 26/2014; Authorization n.19/2008-A issued 6 March 2008 by the Ministry of Health); Mario Negri Institutional Regulations and Policies providing internal authorization for persons conducting animal experiments (Quality Management System Certificate—UNI EN ISO 9001:2015—Reg. No. 6121); the NIH Guide for the Care and Use of Laboratory Animals (2011 edition); and EU directives and guidelines (EEC Council Directive 2010/63/UE). Approval of the study was obtained by the Local Institutional Review Board Committee and governmental institutions (210-2010-B). This study followed Animal Research: Reporting of In Vivo Experiments guidelines.

Experimental design and study animals

The flow chart of this study is summarized in *Figure 1A*. Male Sprague Dawley rats (Envigo, Italy) weighing 483.5 ± 8.2 g were included. The animals were acclimated to housing, food, and water conditions for 4 days before the start of

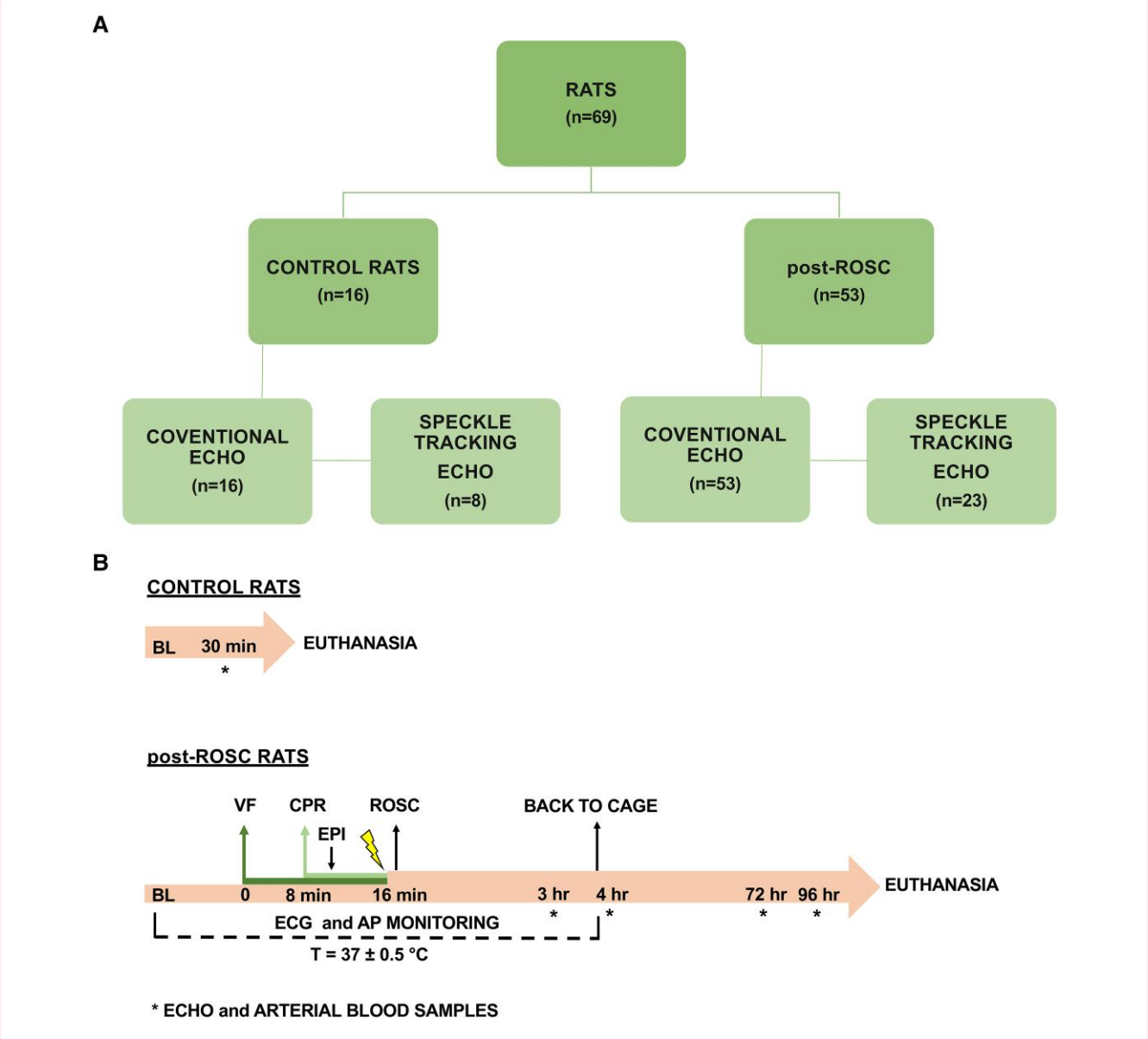

Figure 1 Flow chart of the experimental study (*A*) and experimental outline and procedures (*B*). BL, baseline; ECG, electrocardiogram; AP, arterial pressure; T, temperature.

the experiments, in a specific pathogen-free environment. Rats were co-housed in polycarbonate, solid-bottom cages in a temperature-controlled environment (22 ± 2°C), with 45–65% humidity and 12 h light–dark cycles; they had free access to SDS VRF1 certified pellet diet (Special Diets Services, LBS Biotechnology, UK) and reverse osmosis–filtered water. Animals were fasted overnight except for free access to water before the experiment.

Sixty-nine rats were divided into naïve/control rats ($n = 16$) and animals that underwent 8 min of untreated VF and 8 min of CPR ($n = 53$). Fifty-three of these rats were successfully resuscitated and were studied: $n = 27$ up to 72 h and $n = 26$ up to 96 h.

To follow STE analysis, a subset of 31 rats was considered ($n = 8$, control rats; $n = 23$, post-ROSC rats).

Experimental procedures

The experimental procedures are displayed in *Figure 1B*. Animals were anaesthetized by intraperitoneal injection of pentobarbital (50 mg/kg); additional doses (10 mg/kg) were injected at 1-h intervals or when necessary for the maintenance of general anaesthesia.

The LV function of control rats was assessed by echocardiography immediately after anaesthesia. Afterwards, a blood sample (1.0 mL) was drawn from a cannula inserted into the femoral artery up to the descending aorta.

CA induction was followed as previously reported.[6] Briefly, animals were subjected to 8 min of untreated VF and 8 min of mechanical precordial compression and ventilation before defibrillation; epinephrine (0.02 mg/kg) was injected into the right atrium 2 min after the start of compressions. After resuscitation, rats were invasively monitored for up to 4 h. A blood sample was then drawn, catheters were removed, and an echocardiographic examination was done. Ampicillin (50 mg/kg) and buprenorphine (0.16 mg/kg) were injected before the induction of CA and before returning rats to their cages, to prevent infection and pain after extubation.

Animals were observed up to 72 or 96 h post-ROSC. At the end of the observation period, pentobarbital (45 mg/kg) was injected i.p. before echocardiographic examination.

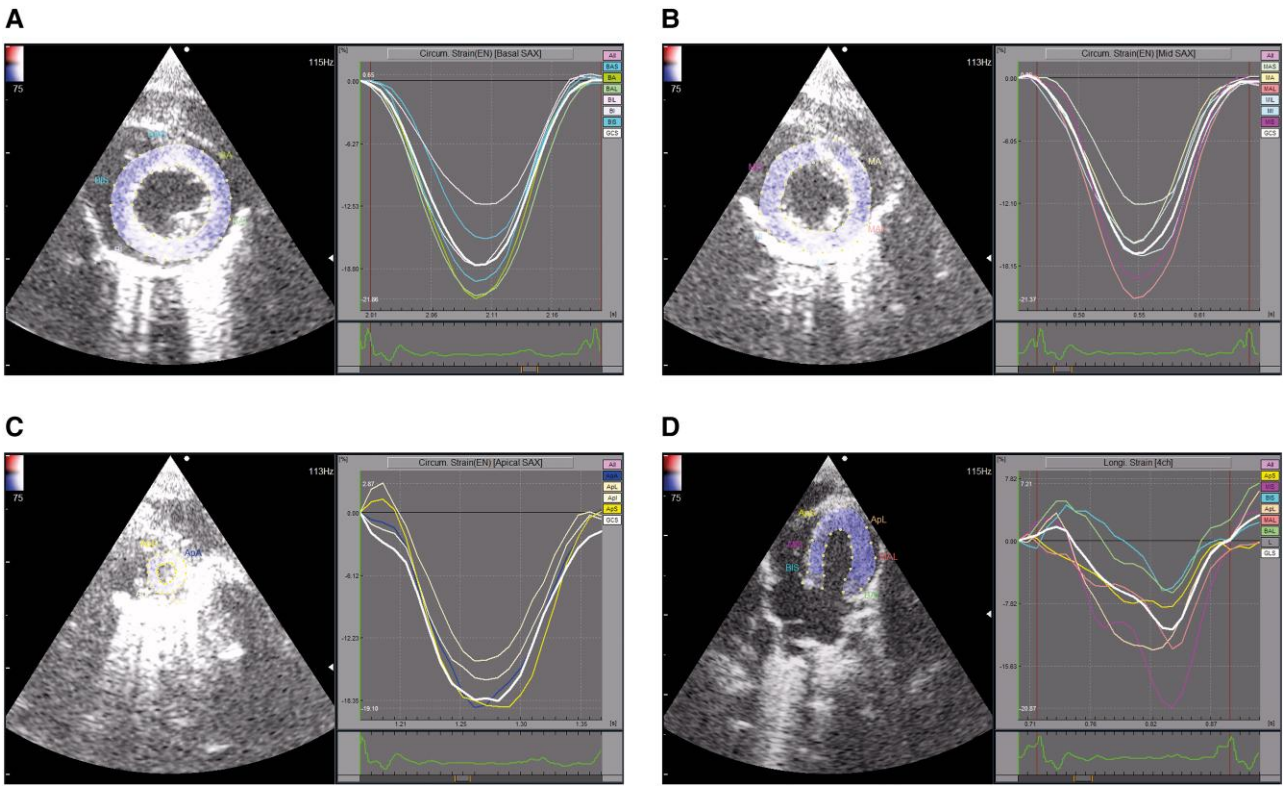

Figure 2 Example of mid-papillary (*A*), sub-papillary (*B*), apical (*C*) CS and longitudinal strain (*D*) in control rats. Curves indicate strain in different segments. BA, mid-papillary anterior; BAS, mid-papillary anteroseptal; BIS, mid-papillary inferoseptal; BI, mid-papillary inferior; BIL, mid-papillary inferolateral; BAL, mid-papillary anterolateral; MA, sub-papillary anterior; MAS, sub-papillary anteroseptal; MIS, sub-papillary infero septal; MI, sub-papillary inferior; MIL, sub-papillary inferolateral; MAL, sub-papillary anterolateral; AA, apical anterior; AS, apical anteroseptal; AI, apical inferior; AL, apical lateral; ApIS, apical inferoseptal; ApL, apicallateral; MIS, mid inferoseptal; MAL, mid anterolateral; BIS, basal inferoseptal; BAL, basal anterolateral.

Echocardiography

Transthoracic echocardiography was done in control rats and in resuscitated rats at 3, 4, 72, and 96 h post-ROSC.

Conventional and speckle-tracking echocardiography (STE) was performed with an Arietta V70 (Hitachi-ALOKA, Japan) machine equipped with a linear high-frame rate imaging transducer, 5–18 MHz, and a 2–9 MHz phased array probe. Three electrocardiographic leads were used to obtain a simultaneous display during the examination. All measurements and calculations were taken in three or five consecutive cardiac cycles and were followed according to the recommendations of the latest American and European Societies Guidelines for echocardiographic assessment,[9–11] as previously reported.[5,6]

Analysing the motion of speckles in the 2D ultrasonic image by STE, we assessed myocardial deformation and quantified myocardial thickening, shortening, and the rotation dynamics of the LV,[12] using a speckle-tracking algorithm provided by Hitachi-ALOKA.

Adequate B-mode cine loops were selected from the digitally acquired echocardiographic session. For circumferential, radial strain and strain rate analyses, mid-papillary, sub-papillary, and apical parasternal short-axis (SAX) views of the LV were acquired, and for longitudinal strain and longitudinal strain rate, apical four-chamber (4APCH) view was obtained (*Figure 2*). LV myocardium in mid-papillary and sub-papillary SAX and 4APCH views was divided into six standard anatomic segments; in the apical SAX view, it was divided into four segments. For all parameters, peak systolic strain was averaged across all segments (*Figure 2*).

LV rotations were determined at the mid-papillary and apical SAX views. In order to use the same views as in conventional echocardiography, the upper SAX view is at mid-papillary level and not at 'the standard base level' at the mitral valve, a reason why we did not measure the total twist. The positive peak of apical and the negative peak of mid-papillary level LV rotations were measured automatically.

All strain measurements were averaged over five cardiac cycles. After selecting an end-systolic frame from each studied view, the investigator manually traced the LV endocardial borders before processing the data with the machine software.

Blood sampling, troponin and natriuretic peptide assays, and euthanasia

After the echo exam in control rats and after 3 or 4 h and 72 or 96 h post-ROSC, blood samples of 0.5 mL were taken with heparinized syringes from the jugular and femoral arteries, respectively. Blood was immediately centrifuged, and plasma was stored at −70°C in 0.2-mL aliquots for subsequent biomarker assays. Plasma high-sensitivity cardiac troponin T (hs-cTnT) was measured with an electrochemiluminescence assay (Cobas, Roche Diagnostics, Rotkreuz, Switzerland). N-terminal pro-atrial natriuretic peptide (NT-proANP) was measured with an ELISA assay (Biomedica BI-20892).[13]

Soon after the last blood sampling, rats were euthanized with an intravenous injection of 150 mg/kg of pentobarbital.

Statistical analysis

All data are reported as mean ± standard error of the mean (SEM). Variables not normally distributed are reported as median and inter-quartile range. Non-parametric Mann–Whitney *U* test and Student's *t*-test were

used, as appropriate; all time points were compared with control rats. Spearman or Pearson correlation coefficient and the corresponding two-sided 95% confidence intervals and *P*-values were calculated to assess the association among hs-cTnT, NT-proANP levels, and each structural and functional cardiac measurement; this analysis was repeated at each time point.

Inter-observer and intra-observer agreements were determined using Bland–Altman analysis to identify possible bias (mean difference between two readings) and the limits of agreement (±2 SD of the mean difference). Data were analysed using GraphPad Prism 9.2 software. A two-tailed *P*-value <0.05 was considered significant.

Results

A total of 68 rats were included, 15 control and 53 post-ROSC rats. Survival at 72 h post-ROSC was 22/27 (81.5%) and at 96 h, 17/26 (64.4%). Body weight (BW) decreased by 10.1% at 72 h and by 12.6% at 96 h post-ROSC (mean control rats BW: 477 ± 6.6 g).

Conventional echocardiographic parameters

Three and 4 h post-ROSC

Heart rate (HR) during echo in animals at 3 and 4 h post-ROSC was similar to that in control rats (see Supplementary data online, *Table S1*).

Compared with control rats, left ventricular end-diastolic and end-systolic volumes (LVEDV and LVESV) were +17.8% higher for 3 h post-ROSC ($P = 0.04$) and +70.0% for 3 and 4 h post-ROSC ($P < 0.0001$), and shortening fraction (SF) and LVEF were significantly lower (SF: −109 and −110%; LVEF: −147 and −155%, $P < 0.0001$ for all). Again, compared with control rats, s′ velocity obtained by Tissue Doppler Imaging (TDI) was lower in both early post-ROSC time points (−43.9 and −73.5%, respectively, $P < 0.001$, for both). In addition, CO and stroke volume (SV) were lower shortly after ROSC than in control rats ($P < 0.0001$ for both; see Supplementary data online, *Table S1*).

Peak mitral E and A waves' velocity by pulsed Doppler was significantly lower at 3 and 4 h compared with control rats ($P < 0.0001$ for both) with a significantly longer duration of isovolumetric relaxation time (IVRT; $P < 0.0001$). At 3 h post-ROSC, the e′ mean velocity by TDI was 21.2% lower than control rats ($P = 0.04$), the difference that became larger at 4 h post-ROSC (−54%, $P = 0.0003$).

Seventy-two and 96 h post-ROSC

Compared with control rats, a 13.2 and 21.1% lower HR was found, respectively, at 72 and 96 h post-ROSC (see Supplementary data online, *Table S1*). At 72 h post-ROSC, SF and LVEF were almost normalized (48.5 ± 2.2 and 74.8 ± 2.4%, respectively) and completely at 96 h (54.7 ± 3.4 and 76.9 ± 3.0%%, respectively). Also, LVEDV and LVESV were normalized (335.2 ± 25.6 and 82.5 ± 9.1 μL at 72 h and 353.4 ± 23.3 and 93.8.5 ± 16.9 μL at 96 h, respectively). Interestingly, while shortly after resuscitation diastolic intra-ventricular septum thickness did not show any difference compared with control rats, it was thicker at 72 h after resuscitation (+18.3%, $P = 0.01$).

TDI showed that the mean s′ wave velocity increased up to 96 h, though mean values remained significantly lower than in control rats. A similar pattern was observed for CO and SV.

E vel and A vel, but not IVRT, improved at 72 and 96 h post-ROSC.

STE in control rats

The mean values of STE variables in control rats are reported in Supplementary data online, *Table S2* and *Figures 3* and *4*.

Circumferential strain

LV global circumferential strain (CS) was −14.1 ± 0.7% and decreased from the mid-papillary level towards the sub-papillary and apical levels (−13.0 ± 1.3, −14.9 ± 1.0, and −14.3 ± 1.1, respectively).

CS rate

LV global CS rate (GCSR) in control rats was −5.0 ± 0.1 and was lowest at the apex.

Radial strain

The peak of radial systolic strain increased from the mid-papillary and sub-papillary levels towards the apex (4.7 ± 0.6, 4.1 ± 0.8, and 7.8 ± 1.2, respectively).

Radial strain rate

Radial strain rate also increased from the mid-papillary level (1.0 ± 0.2/s) to the sub-papillary level (1.2 ± 0.2/s) and the apex (1.7 ± 0.1/s).

Longitudinal strain

The LV longitudinal strain was −11.0 ± 1.2%.

Longitudinal strain rate

The global longitudinal strain rate (GLSR) was −2.3 ± 0.2/s.

LV rotations at mid-papillary and apical levels

The mean LV rotation was −0.4 ± 0.4° at the mid-papillary level and 2.4 ± 0.4° at the apex.

STE post-ROSC

Three and 4 h post-ROSC

At 3 and 4 h post-ROSC, global CS (GCS) and global longitudinal strain (GLS) were significantly higher than in control rats, and global radial strain was significantly lower (see Supplementary data online, *Table S2*; *Figure 3*).

At 3 and 4 h post-ROSC, all segments studied had higher peak systolic CS ($P < 0.01$ vs. control rats; see Supplementary data online, *Table S2*; *Figure 3*).

At 3 and 4 h post-ROSC, mainly the interventricular septum (IVS), the anterolateral and lateral walls presented segments with increased longitudinal strain (LS) values (see Supplementary data online, *Table S2*; *Figure 4*).

GCSR and GLSR 3 and 4 h post-ROSC were significantly different from those in control rats ($P < 0.0001$ for both; see Supplementary data online, *Table S2*).

At 3 and 4 h post-ROSC, LV mid-papillary and apical rotations were 35% and 50 higher than in control rats, but the differences were not significant due to a high inter-individual variability (see Supplementary data online, *Table S2*).

Seventy-two and 96 h post-ROSC

At 72 and 96 h post-ROSC, GCS and radial strail (RS) were similar to those in control rats (see Supplementary data online, *Table S2*; *Figures 5*).

GLS was still abnormal at 72 and 96 h post-ROSC (−5.9 ± 0.7%, $P = 0.001$ and −7.5 ± 0.5%, $P = 0.04$, respectively, vs. control rats). At 72 h post-ROSC, four of six segments were still affected, and at 96 h, two of six segments were still affected (see Supplementary data online, *Table S2*; *Figure 5*). GLSR was also higher at 72 and 96 h post-ROSC compared with control rats (−1.3 ± 0.2/s^{-1}, $P = 0.001$, and −0.9 ± 0.4/s, $P = 0.02$, respectively); segments from septal and lateral walls were still impaired (see Supplementary data online, *Table S2*).

An inverse correlation was found at 96 h post-ROSC between GLS and two variables that assess LV filling velocity: E vel ($\rho = -87$, $P = 0.05$;

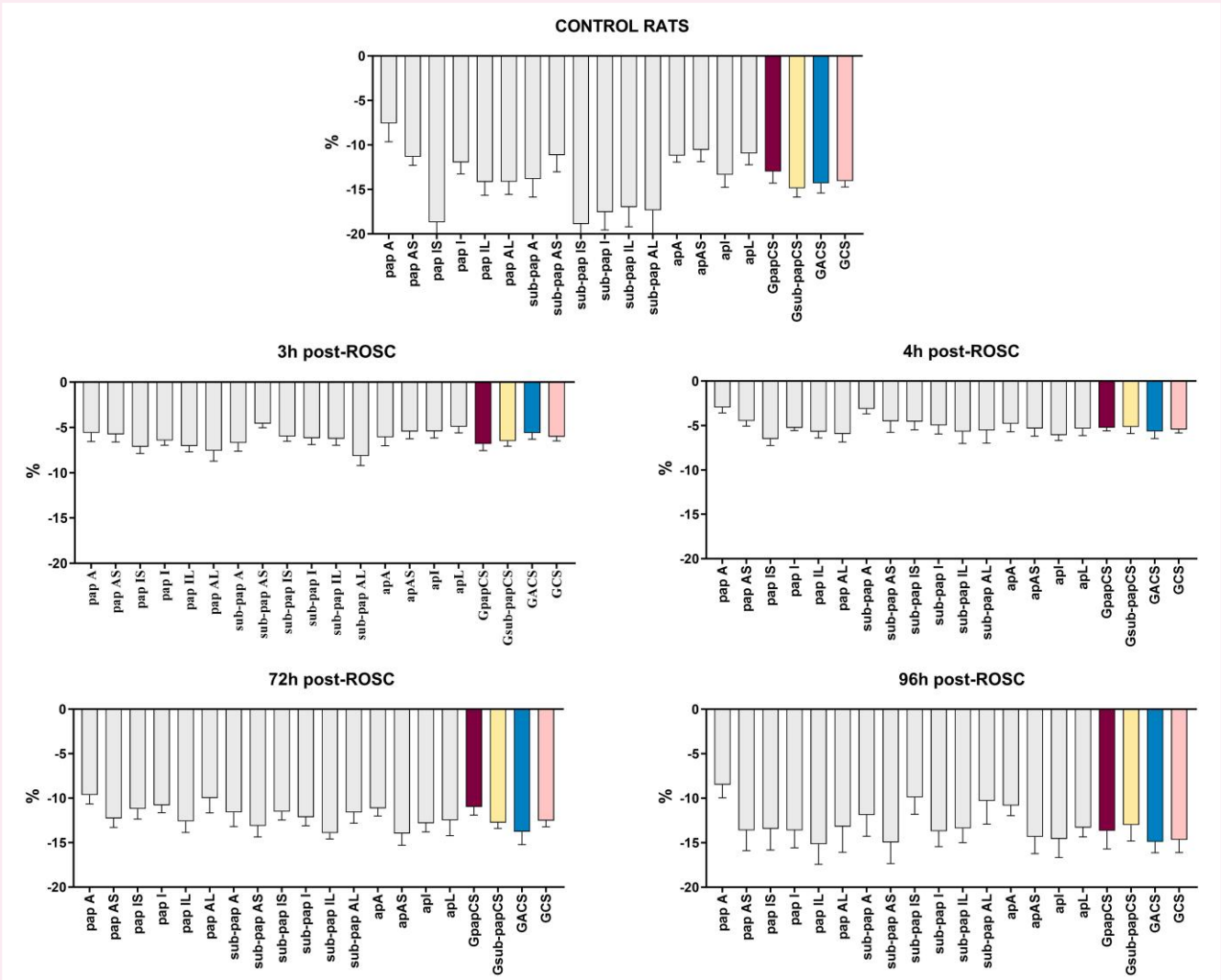

Figure 3 GCS and segmental CS in control rats and at 3, 4, 72, and 96 h post-ROSC. Data are mean ± SEM, $n = 8$ for control rats and $n = 6$–11 for post-ROSC rats. pap A, mid-papillary anterior; pap AS, mid-papillary anteroseptal; pap IS, mid-papillary inferoseptal; pap I, midpapillary inferior; pap IL, mid-papillary inferolateral; pap AL, mid-papillary anterolateral; sub-pap A, sub-papillary anterior; sub-pap AS, sub-papillary antero-septal; sub-pap IS, sub-papillary inferoseptal; sub-pap I, sub-papillary inferior; sub-pap IL, sub-papillary inferolateral; sub-pap AL, sub-papillary anterolateral; ap A, apical anterior; ap AS, apical antero-septal; ap I, apical inferior; ap L, apical lateral; GpapCS, global papillary CS; Gsub-papCS, global sub-papillary CS; GACS, global apical CS.

see Supplementary data online, *Figure S1A*) and A vel ($\rho = -0.92$, $P = 0.03$; see Supplementary data online, *Figure S1B*).

Inter-observer and intra-observer variability

The inter-observer and intra-observer reproducibility of GCS, GLS, and GLSR in control rats and 72 and 96 h post-ROSC rats (see Supplementary data online, *Table S3*) showed that in both conditions, measures were reproducible.

hs-cTnT and NT-proANP concentrations post-ROSC

In resuscitated rats 3 and 4 h post-ROSC, hs-cTnT plasma concentration was significantly elevated [median (Q1–Q3) 5102 (3903–5979) and 6808 (5494–10.000) ng/L, respectively, $P < 0.0001$ for both compared with control rats, 64 (42–98) ng/L]; those were normal at 96 h post-ROSC [70 (48–115) ng/L]. hs-cTnT concentration was highest at 4 h post-ROSC.

NT-proANP also increased 3 and 4 h after ROSC [median (Q1–Q3) 2.2 (1.7–3.2) and 3.3 (1.6–4.3) nmol/L, respectively, vs. 0.4 (0.2–0.8) nmol/L in control rats, $P < 0.0001$], and for NT-proANP, the concentration was highest 4 h post-ROSC. At 72 and 96 h post-ROSC, the NT-proANP concentration was still high [2.5 (1.4–4.6) nmol/L at both time points].

A significant inverse correlation was found 96 h post-ROSC between NT-proANP and two variables that assess LV filling velocity: peak E vel ($\rho = -0.70$, $P = 0.003$; see Supplementary data online, *Figure S2A*) and A vel ($\rho = -0.55$, $P = 0.03$; see Supplementary data online, *Figure S2B*). No correlations were found between echocardiographic variables and hs-cTnT.

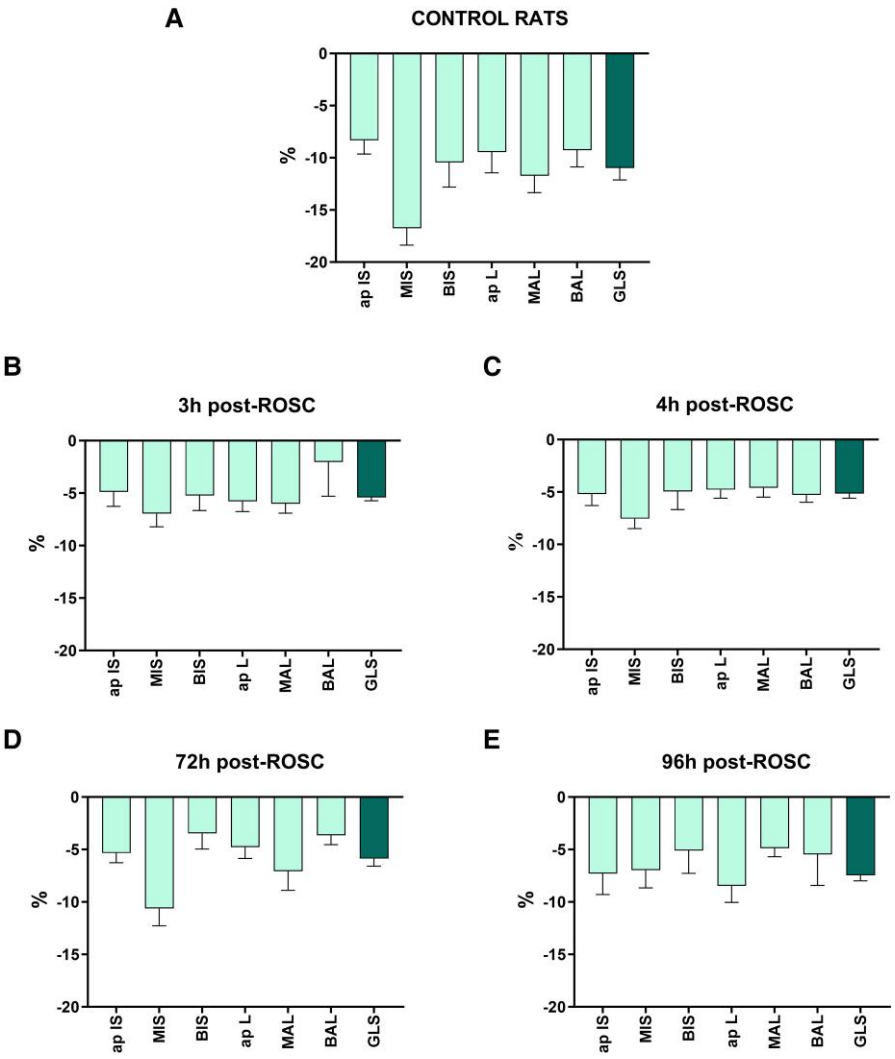

Figure 4 Example of longitudinal strain in control rats (*A*) and at 3 (*B*), 4 (*C*), 72 (*D*) and 96 (*E*) h post-ROSC. Lines represent different segments. ApIS, apical inferoseptal; ApL, apical lateral; MIS, mid inferoseptal; MAL, mid anterolateral; BIS, basal inferoseptal; BAL, basal anterolateral.

Discussion

To our knowledge, this study is the first to show that LV function in rats does not recover completely 96 h post-ROSC even if LVEF normalizes. This finding is supported by the persistence of abnormal s′ mean wave velocity by TDI and GLS and GLSR values by STE together with the persistently high NT-proANP concentration, indicating a lasting cardiomyocyte injury and increased intracardiac chamber pressure and stress 96 h post-ROSC.

Post-CA syndrome is characterized by myocardial dysfunction due to cardiac I/R injury. When a short period of ischaemia is relieved by reperfusion, the myocardium is viable but presents transient post-ischaemic contractile and biochemical dysfunction, called stunning.[14] Post-ROSC reversible myocardial dysfunction was described for the first time in pigs in which LVEF decreased 30 min post-ROSC from normal value to ∼20% and then improved at 24 h and finally normalized within 48 h.

Various experimental studies describe early changes in LV function, by conventional echocardiography, in a rat model of CA (see Supplementary data online, *Table S4*). The echocardiographic variables reported in these studies depicted an impaired myocardial systolic function based on LVEF and CO at baseline and 4 h post-ROSC, in agreement with the results reported in this study and in our previous work.[6]

In the present study, we followed the time course of myocardial dysfunction until 96 h post-ROSC through extensive echocardiographic evaluation of LV systolic and diastolic functions, combining different echo methods including STE and assessing cardiac biomarkers plasma concentration.

At 72 and 96 h post-ROSC, although CO, SV, and s′ wave velocity increased, they did not reach levels similar to those in control rats. Moreover, IVRT remained significantly longer, indicating the persistent enhancement of LV relaxation. All these results suggest either a longer recovery phase or that myocardial dysfunction in this established model of CA may not be fully reversible, as previously suggested.[15] The explanation may lie in the fact that residual alterations of myocardial function are subtle enough to require the high sensitivity of STE to be detected. The inverse relation between E and A trans-mitral flow velocities with NT pro-ANP plasma levels (see Supplementary data online, *Figure S1A and B*) and GLS (see Supplementary data online, *Figure S2A and B*) may indicate an increase in LV filling pressure 96 h post-ROSC.

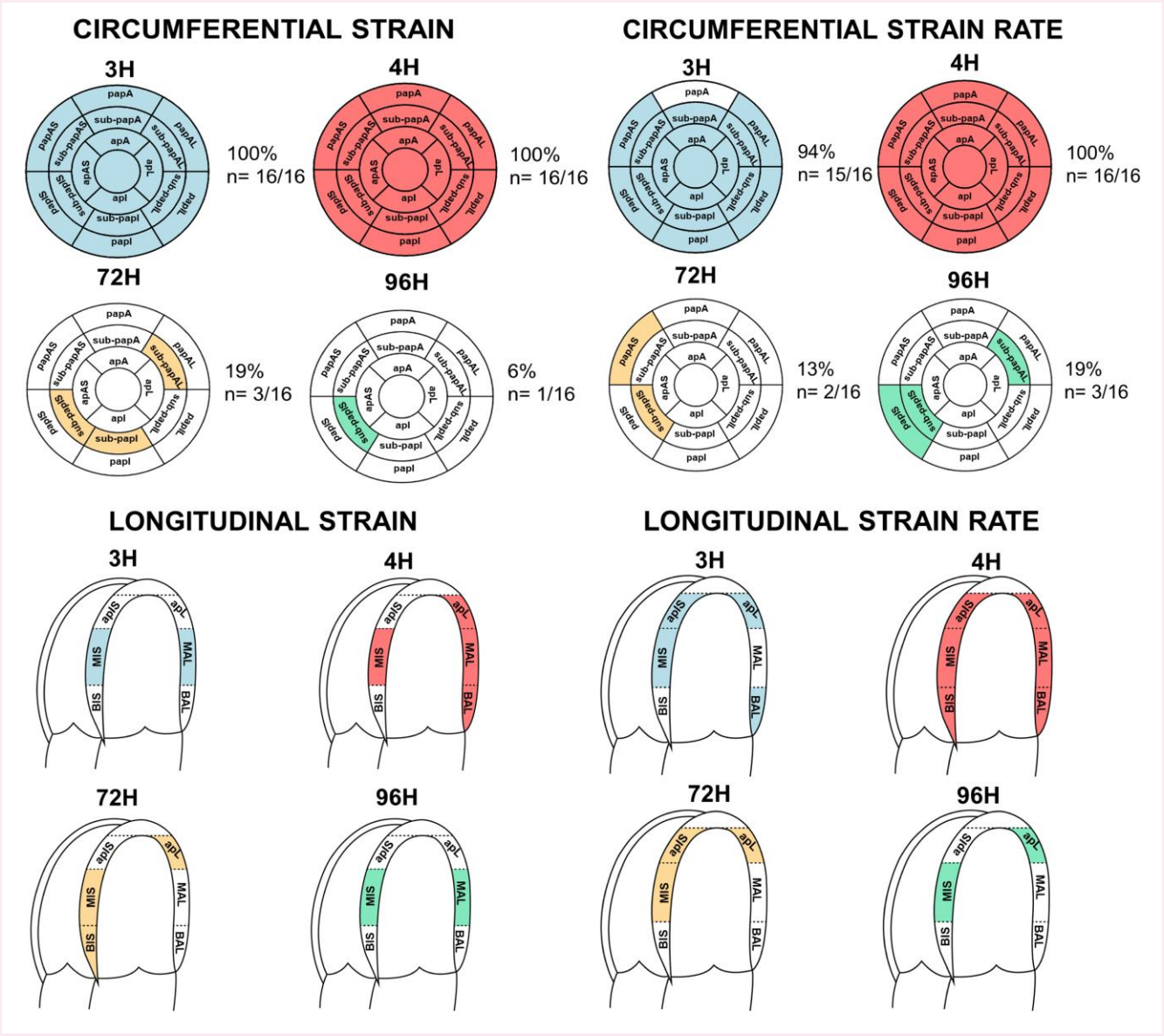

Figure 5 Compromised LV segments were assessed by CS and longitudinal strain and strain rate at 3, 4, 72, and 96 h post-ROSC. pap A, mid-papillary anterior; pap AS, mid-papillary anteroseptal; pap IS, mid-papillary inferoseptal; pap I, mid-papillary inferior; pap IL, mid-papillary inferolateral; pap AL, mid-papillary anterolateral; sub-pap A, sub-papillary anterior; sub-pap AS, sub-papillary antero-septal; sub-pap IS, sub-papillary inferoseptal; sub-pap I, sub-papillary inferior; sub-pap IL, sub-papillary inferolateral; sub-pap AL, sub-papillary anterolateral; ap A, apical anterior; ap AS, apical antero-septal; ap I, apical inferior; ap L, apical lateral; ApIS, apical inferoseptal; ApL, apical lateral; MIS, mid inferoseptal; MAL, mid anterolateral; BIS, basal inferoseptal; BAL, basal anterolateral. All segments highlighted in different colours represent compromised. The number of segments that represent compromised are shown beside each figure.

STE measures myocardial motion in any direction against a fixed external point, so it can identify the deformation of myocardial tissue in three planes. Strain rate measures the time course of myocardial deformation and is closely correlated with the ratio of pressure change in the ventricular cavity during isovolaemic contraction, a readout of LV contractility.[16]

The sub-endocardial layer of the myocardium is characterized by a mixture of high energy expenditure and borderline level of perfusion since it is the farthest point from the coronary supply of blood; these proprieties make it more vulnerable to injury and compression[17] GLS reflects the function of longitudinally oriented sub-endocardial muscle fibres[18,19]; as described for other cardiac diseases with sub-endocardial involvement,[20,21] the probability to detect persistent myocardial injury post-ROSC lies mostly in GLS and not in CS and RS.

GLS and GLSR were still impaired 72 h post-ROSC and less so at 96 h; this can be at least partly attributed to later recovery of the IVS and lateral wall since regional abnormalities were identified (*Figure 5*; see Supplementary data online, *Table S2*). To our knowledge, only one previous study[22] reported in a VF CA model in piglets studied with magnetic resonance imaging 4 h post-ROSC regional LV wall motion abnormalities in the territory of the left anterior descendent artery without a difference in myocardial perfusion parameters. As for these authors, we do not know the reasons and the mechanisms of this finding.

LV function is influenced by complex interactions among tissue anatomy, myocardial contractility, and LV loading conditions, and the CA model in rats is an example of multi-faceted changes in cardiac structure and function. In our study, at 72 h post-ROSC, the posterior wall and, particularly, the IVS were significantly thicker in some animals, probably due to the persistence of the stunned myocardium. At the same time, the decreased LV dimensions and LV filling (low E and A velocities CO and SV; see Supplementary data online, *Table S1*) may also probably have been due to the animal's lower capacity for self-hydration after CA.[23,24] Some variables indicated compromised LV diastolic function as a significantly longer deceleration time and IVRT and a mean E/e' ratio of 18.6 ± 1.0; at 96 h, some of these parameters normalized and others improved with the exception of IVRT. The discrepancy between the normalization of LVEF after 72 and 96 h post-ROSC and other systolic and diastolic variables still altered, suggested the assessment of myocardial global and regional contractility with a more sensible echocardiographic methodology.

Strengths and limitations

Our results are based on a validated and reliable animal model of CA, which is in line with previous studies[3,4,8,15] (see Supplementary data online, *Table S4*). Moreover, the present results greatly represent the transient phenomenon of LV dysfunction in the post-CA syndrome observed also in patients,[25] and our data were in line with previous studies using the same rat model of CA. Echocardiography, a non-invasive, consistent, and clinically accepted tool was used to describe cardiac function and myocardial deformation before and after CA in a pre-clinical setting at short-term and mid-term time points. However, to select the fittest CA model to test therapeutic drugs, a full echocardiographic examination of the LV is necessary to evaluate LV systolic and diastolic dysfunctions after CA.

It is widely accepted that conventional and STE echocardiographies have several advantages over other imaging techniques such as cardiac magnetic resonance imaging. The advantages are as follows: the lower cost, greater accessibility, less time consuming, and a large number of animals can be studied at different times in order to better assess the progression of a disease.

However, there are certain limitations. Our rat model, previously validated by von Planta *et al.*,[26] requires 30-min interval between the last injection of pentobarbital and the induction of VF in order to minimize any cardio-depressant effect that may interfere with successful resuscitation. Since 30 min is not always sufficient to perform a complete transthoracic echocardiographic examination like the ones followed in our study, we chose to include a control group of naïve animals instead of performing an echo exam at baseline before CA induction.

In humans and rats, myocardial dysfunction was associated with the number of defibrillations, cumulative doses of epinephrine during resuscitation, and total resuscitation time.[27,28] In the present study, 50% of rats with severe LV systolic dysfunction (LVEF ≤30%) at 3 or 4 h post-ROSC received ≥2 shocks (range 2–8) and ≥4 J (range 4–13 J) of energy for defibrillation.

It is noted that intact rats present STE values similar to those in humans, and even the orientation of the contractile fibres is comparable, with segmental heterogeneity, observed by Bachner-Hinenzon *et al.*[29] and confirmed in our study (see Supplementary data online, *Table S2*). Moreover, LS was measured from the 4APCH view and not from the parasternal long-axis as in other studies[29] aiming to avoid the LV foreshortening in the apical view in rats. We could not obtain the parasternal long-axis view since the phase array probe, useful for strain imaging, does not allow the inclusion of the apex.

Conclusion

More sensitive echocardiographic parameters other than LVEF, TDI s' velocity, and GLS and GLSR showed that LV systolic function is still impaired 96 h after resuscitation. This is in accordance with the NT-proANP concentration that was still high. Further investigations are needed to provide more evidence in the progression of post-ROSC LV diastolic function.

Supplementary data

Supplementary data are available at *European Heart Journal - Imaging Methods and Practice* online.

Acknowledgements

We are grateful to Judith Baggott for language editing and Alice Salimbeni for figure preparation.

Author contributions

All authors had full access to all the data and took responsibility for its integrity and the accuracy of data analysis. L.S., D.D.G., and R.L.: study concept and design. L.S., D.D.G., G.R., and R.L: data acquisition, analysis, or interpretation. L.S., D.D.G., and R.L.: drafting the manuscript. D.D.G., D.O., D.N., F.F., F.M., M.C., G.R., R.L., and L.S.: critical revision of the manuscript for important intellectual content. D.D.G. and L.S.: statistical analysis. All authors contributed to revision of the manuscript and accepted the final version.

Conflict of interest: None declared.

Funding

None declared.

Data availability

The data underlying this article will be shared on reasonable request to the corresponding author.

Lead author biography

Daria De Giorgio had her master degree in Medical Biotechnology at the Università degli Studi di Milano-Bicocca. She is now a PhD student at the Open University (Milton Keynes, UK), conducting her research activity at Istituto di Ricerche Farmacologiche Mario Negri IRCCS. She is performing *in vivo* experiments on animal models of myocardial infarction and cardiac arrest, with corroborated experience in experimental transthoracic echocardiography. During her early career, she had the opportunity to attend several international scientific conferences and to become member of the European Society of Intensive Care Medicine (ESICM) and of the Italian Resuscitation Council (IRC) working groups.

References

1. Tsao CW, Aday AW, Almarzooq ZI, Anderson CAM, Arora P, Avery CL *et al.* Heart disease and stroke statistics—2023 update: a report from the American Heart Association. *Circulation* 2023;**147**:e93–621.
2. Nolan JP, Sandroni C, Böttiger BW, Cariou A, Cronberg T, Friberg H *et al.* European Resuscitation Council and European Society of Intensive Care Medicine guidelines 2021: post-resuscitation care. *Intensive Care Med* 2021;**47**:369–421.

3. Uray T, Lamade A, Elmer J, Drabek T, Stezoski JP, Missé A *et al.* Phenotyping cardiac arrest: bench and bedside characterization of brain and heart injury based on etiology. *Crit Care Med* 2018;**46**:e508–15.
4. El-Menyar AA. The resuscitation outcome. *Chest* 2005;**128**:2835–46.
5. Fumagalli F, Russo I, Staszewsky L, Li Y, Letizia T, Masson S *et al.* Ranolazine ameliorates postresuscitation electrical instability and myocardial dysfunction and improves survival with good neurologic recovery in a rat model of cardiac arrest. *Heart Rhythm* 2014;**11**: 1641–7.
6. Lucchetti J, Fumagalli F, Olivari D, Affatato R, Fracasso C, De Giorgio D *et al.* Brain kynurenine pathway and functional outcome of rats resuscitated from cardiac arrest. *J Am Heart Assoc* 2021;**10**:e021071.
7. Lu X, Ma L, Sun S, Xu J, Zhu C, Tang W. The effects of the rate of postresuscitation rewarming following hypothermia on outcomes of cardiopulmonary resuscitation in a rat model. *Crit Care Med* 2014;**42**:e106–13.
8. Chung SP, Song F-Q, Yu T, Weng Y, Sun S, Weil MH *et al.* Effect of therapeutic hypothermia vs δ-opioid receptor agonist on post resuscitation myocardial function in a rat model of CPR. *Resuscitation* 2011;**82**:350–4.
9. Quiñones MA, Otto CM, Stoddard M, Waggoner A, Zoghbi WA. Recommendations for quantification of Doppler echocardiography: a report from the Doppler quantification task force of the nomenclature and standards committee of the American Society of Echocardiography. *J Am Soc Echocardiogr* 2002;**15**:167–84.
10. Nagueh SF, Smiseth OA, Appleton CP, Byrd BF, Dokainish H, Edvardsen T *et al.* Recommendations for the evaluation of left ventricular diastolic function by echocardiography: an update from the American Society of Echocardiography and the European Association of Cardiovascular Imaging. *Eur Heart J Cardiovasc Imaging* 2016;**17**:1321–60.
11. Lang RM, Badano LP, Mor-Avi V, Afilalo J, Armstrong A, Ernande L *et al.* Recommendations for cardiac chamber quantification by echocardiography in adults: an update from the American Society of Echocardiography and the European Association of Cardiovascular Imaging. *J Am Soc Echocardiogr* 2015;**28**:1–39.e14.
12. Voigt J-U, Pedrizzetti G, Lysyansky P, Marwick TH, Houle H, Baumann R *et al.* Definitions for a common standard for 2D speckle tracking echocardiography: consensus document of the EACVI/ASE/Industry Task Force to standardize deformation imaging. *J Am Soc Echocardiogr* 2015;**28**:183–93.
13. Vinken P, Reagan WJ, Rodriguez LA, Buck WR, Lai-Zhang J, Goeminne N *et al.* Cross-laboratory analytical validation of the cardiac biomarker NT-proANP in rat. *J Pharmacol Toxicol Methods* 2016;**77**:58–65.
14. Kern KB, Hilwig RW, Rhee KH, Berg RA. Myocardial dysfunction after resuscitation from cardiac arrest: an example of global myocardial stunning. *J Am Coll Cardiol* 1996; **28**:232–40.
15. Ruiz-Bailén M, de Hoyos EA, Ruiz-Navarro S, Díaz-Castellanos MÁ, Rucabado-Aguilar L, Gómez-Jiménez FJ *et al.* Reversible myocardial dysfunction after cardiopulmonary resuscitation. *Resuscitation* 2005;**66**:175–81.
16. Cameli M. Echocardiography strain: why is it used more and more? *Eur Heart J Suppl* 2022;**24**(Suppl I):I38–42.
17. Heusch G. Myocardial ischemia: lack of coronary blood flow or myocardial oxygen supply/demand imbalance? *Circ Res* 2016;**119**:194–6.
18. Greenbaum RA, Ho SY, Gibson DG, Becker AE, Anderson RH. Left ventricular fibre architecture in man. *Br Heart J* 1981;**45**:248–63.
19. Stanton T, Marwick TH. Assessment of subendocardial structure and function. *JACC Cardiovasc Imaging* 2010;**3**:867–75.
20. Zhang K, Sheu R, Zimmerman NM, Alfirevic A, Sale S, Gillinov AM *et al.* A comparison of global longitudinal, circumferential, and radial strain to predict outcomes after cardiac surgery. *J Cardiothorac Vasc Anesth* 2019;**33**:1315–22.
21. Slivnick JA, Singulane C, Sun D, Eshun D, Narang A, Mazzone S *et al.* Preservation of circumferential and radial left ventricular function as a mitigating mechanism for impaired longitudinal strain in early cardiac amyloidosis. *J Am Soc Echocardiogr* 2023;**36**:1290–301.
22. Venkata GK, Forder JR, Clark D, Shih A, Udassi S, Badugu S *et al.* Ventricular fibrillation-induced cardiac arrest results in regional cardiac injury preferentially in left anterior descending coronary artery territory in piglet model. *Biomed Res Int* 2016; **2016**:5958196.
23. Appleton CP, Hatle LK, Popp RL. Relation of transmitral flow velocity patterns to left ventricular diastolic function: new insights from a combined hemodynamic and Doppler echocardiographic study. *J Am Coll Cardiol* 1988;**12**:426–40.
24. Thomas L, Marwick TH, Popescu BA, Donal E, Badano LP. Left atrial structure and function, and left ventricular diastolic dysfunction. *J Am Coll Cardiol* 2019;**73**:1961–77.
25. Jentzer JC, Anavekar NS, Mankad SV, White RD, Kashani KB, Barsness GW *et al.* Changes in left ventricular systolic and diastolic function on serial echocardiography after out-of-hospital cardiac arrest. *Resuscitation* 2018;**126**:1–6.
26. von Planta I, Weil MH, von Planta M, Bisera J, Bruno S, Gazmuri RJ *et al.* Cardiopulmonary resuscitation in the rat. *J Appl Physiol* 1988;**65**:2641–7.
27. DiCola VC, Freedman GS, Downing SE, Zaret BL. Myocsrdial uptake of technetium-99m stannous pyrophosphate following direct current transthoracic countershock. *Circulation* 1976;**54**:980–6.
28. Yao Y, Johnson NJ, Perman SM, Ramjee V, Grossestreuer AV, Gaieski DF. Myocardial dysfunction after out-of-hospital cardiac arrest: predictors and prognostic implications. *Intern Emerg Med* 2018;**13**:765–72.
29. Bachner-Hinenzon N, Ertracht O, Leitman M, Vered Z, Shimoni S, Beeri R *et al.* Layer-specific strain analysis by speckle tracking echocardiography reveals differences in left ventricular function between rats and humans. *Am J Physiol Heart Circ Physiol* 2010;**299**:H664–72.